Free space TEM transmission lines radiation losses model

Reuven Ianconescu

Shenkar College of Engineering and Design 12, Anna Frank St., Ramat Gan, Israel[*]

Vladimir Vulfin

Department of Electrical and Computer Engineering,

Ben-Gurion University of the Negev, Beer Sheva 84105, Israel[†]

There are three kind of losses in transmission lines: ohmic, dielectric and radiation losses. While the first two are local phenomena which are easy to model, the radiation losses lack a simple model. This work analyzes the radiation losses from two conductors transmission lines in free space, and derives a radiation model within the RLCG transmission lines model.

Keywords: guided EM waves, RLCG model, radiation losses model

[*]Electronic address: riancon@gmail.com,riancon@shenkar.ac.il

[†]Electronic address: vlad2042@yahoo.com

I. INTRODUCTION

While ohmic and dielectric losses in transmission lines (TL) have a simple RLCG telegraph model due to their local characteristics, there is no simple radiation losses model for TL.

The aim of this work is to analyze the radiation process in two conductors TL in free space with the scope of incorporating the radiation losses phenomenon into the RLCG model of the TL. Some preliminary results have been presented in [1].

The methodology we use is the same one used to calculate any small losses: we use the lossless (0'th order solution) for the electric current to derive the losses. This methodology is used to derive the ohmic and dielectric losses [2, 3], and the same approach is used in different radiation schemes from free electrons: one uses the 0'th order current (which is unaffected by the radiation) to calculate the radiation [4, 5]. Corrections to the 0'th order current are not considered in this work.

In section II we present a short review on ohmic and dielectric losses, and show that the RLCG model is accurate only for separate forward or backward waves, while in the case both waves coexist, the interference between them results in an additional losses term.

In section III we define the cross section configuration for the TL that we analyze and show that any open cross section can be modeled in the far field by a twin lead TL, i.e. parallel wires separated by an equivalent distance d. For close cross sections (like the coaxial cable), this equivalent separation $d = 0$, and they practically do not radiate.

In section IV we analyze an infinite TL and show that there is not radiate power (per length unit), ignoring nearby objects which can interfere with the fields. This suggests that radiation from TL must emerge from the termination, in analogy with Optical Transition Radiation (OTR) [6, 7].

In section V we calculate the power radiated by a semi-infinite TL carrying a wave traveling toward the termination and find that it is proportional to the frequency squared times d^2 (the TL length has no effect, being infinite). We also show that the radiated power results are identical for the case of a single wave traveling into the termination or out of the termination, while in the case of a combination of waves their radiated powers add up, so that the interference between the waves has no contribution.

In section VI we calculate the power radiated by a finite line of length $2L$ carrying a

forward wave. We find that for small L the radiation power increases like L^2 and for big L it just tends to a constant which is twice the power radiated by a semi-infinite TL carrying a forward wave, as expected. For a combination of waves, their powers just add up as in the case of the semi-infinite TL.

In section VII we compare the analytic results of section VI with simulation results of the ANSYS-HFSS commercial software. The simulation overestimate the analytic results but show the general tendency of the radiated power to go to a constant with the increase of the TL length. In section VIII we derive the RLCG model for the radiation losses, which requires a series radiation resistance per length unit R which starts at a termination and varies along the TL. The work is ended with some concluding remarks.

Note: through this work, we use RMS values, hence there is no 1/2 in the expressions for power.

II. REMARKS ON OHMIC AND DIELECTRIC LOSSES

The ohmic and dielectric losses are easily incorporated into the RLCG "telegraph" model, so that the ohmic loss per length unit is given by $|I(z)|^2 R$ and the dielectric losses per length unit is given by $|V(z)|^2 G$, where $V(z)$ and $I(z)$ are the voltage and current along the TL. Also one defines the ohmic and dielectric decay coefficients as $\alpha_c = R/(2Z_0)$ and $\alpha_d = GZ_0/2$, Z_0 being the characteristic TL impedance.

However, for unmatched TL, i.e. in presence of both forward and backward moving waves, one has to be careful in evaluating the total ohmic or dielectric losses on the line. For example, let us consider ohmic losses, for the current

$$I(z) = I^+(0)e^{-j\beta z}e^{-\alpha_c z} + I^-(0)e^{j\beta z}e^{\alpha_c z} \tag{1}$$

in a TL from $z = -l/2$ to $z = l/2$. The ohmic losses are

$$\Delta P_c = R\int_{-l/2}^{l/2} |I(z)|^2 = [P^+(0) + P^-(0)][e^{\alpha_c l} - e^{-\alpha_c l}] - 4\alpha_c l P^+(0)\,\mathrm{sinc}(\beta l) Re\{\Gamma(0)\} \tag{2}$$

where $P^{\pm}(0)$ is the power of the forward/backward wave at $z = 0$, respectively, so the first part of the result represents the individual losses of forward/backward waves. The second part represents the contribution of the interference between the waves, and vanishes in some special cases like the length l is an integer multiple of half wavelengths, or the phase of

$\Gamma(0) \equiv -I^-(0)/I^+(0)$ is $\pm\pi/2$, i.e. $|I(z)|^2$ is an anti-symmetric function of z. The "sinc" function in Eq. (2) is defined

$$\mathrm{sinc}(x) \equiv \sin x/x \tag{3}$$

The dielectric losses in presence of both forward and backward waves give a result similar to (2) with α_c replaced by α_d.

Hence the RLCG model for ohmic or dielectric losses, is accurate for a separate forward or backward wave and in presence of both waves the interference between them adds an additional term, which can be positive or negative.

We attempt in this work to derive a similar model for radiation losses, and in the next section we define the cross section configuration on which we shall derive our results.

III. CONFIGURATION

We deal in this work with a two conductor transmission line having a well defined separation between the conductors, as shown in Figure 1. Considering the conductors in free space, a forward wave evolves according to e^{-jkz} at zero order (neglecting the radiation losses, as mentioned in the introduction), hence in the far field the z directed magnetic potential vector A_z due to a forward wave in the transmission line is expressed as

$$A_z = \mu_0 \int_{z_1}^{z_2} dz' \oint dc\, K_z(c) e^{-jkz'} G(R) \tag{4}$$

where the dz' integral goes on the whole length of the TL,

$$G(s) = \frac{e^{-jks}}{4\pi s} \tag{5}$$

is the 3D Green's function, K_z is the surface current distribution as function of the contour parameter c (i.e. c_1 and c_2, see Figure 1) and R is the distance from the integration point on the contour of the conductors to the observer:

$$R = \sqrt{(x - x'(c))^2 + (y - y'(c))^2 + (z - z')^2}. \tag{6}$$

Changing variable

$$z'' = z' - z \tag{7}$$

in Eq. (4), one obtains

$$A_z = \mu_0 e^{-jkz} \int_{z_1 - z}^{z_2 - z} dz'' \oint dc\, K_z(c) e^{-jkz''} G(R), \tag{8}$$

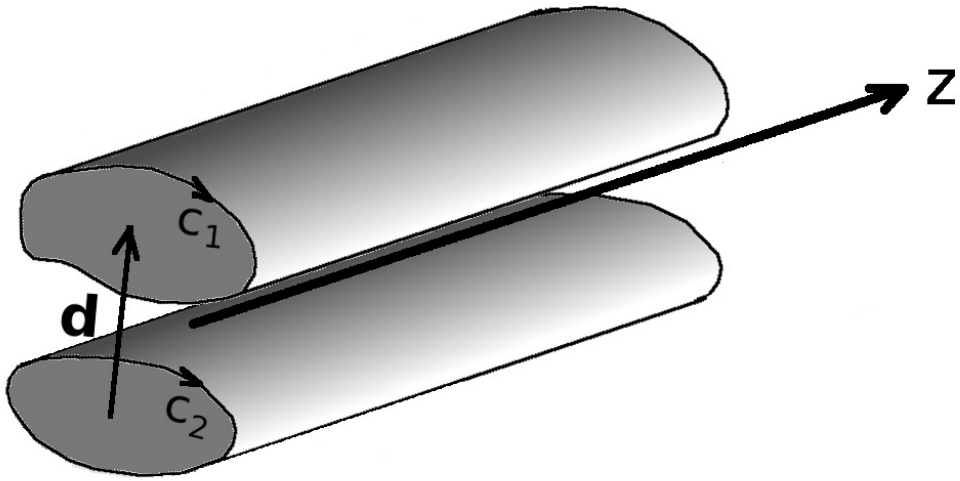

FIG. 1: A basic configuration of a two conductor TL, with a well defined separation between the conductors. The surface current distributions on the contours of the conductors is known from electrostatic considerations, and the total current is the same on both conductors but with opposite signs. The arrow shows the vector distance between the center of the surface current distributions, named **d** and $c_{1,2}$ are the contours of the "upper" and "lower" conductors, respectively.

redefining

$$R = \sqrt{(x - x'(c))^2 + (y - y'(c))^2 + (z'')^2}. \tag{9}$$

For a far observer, at distance $\rho \equiv \sqrt{x^2 + y^2}$ from the TL, so that ρ is much bigger than the transverse dimensions of the TL one approximates R in cylindrical coordinates as

$$R \simeq r - \frac{\rho}{r}\left[x'(c)\cos\varphi + y'(c)\sin\varphi\right], \tag{10}$$

where

$$r(z'') \equiv \sqrt{(z'')^2 + \rho^2}. \tag{11}$$

Using this in Eq. (4), one obtains

$$A_z = \mu_0 e^{-jkz}\int_{z_1-z}^{z_2-z} dz'' \frac{e^{-jk[z''+r(z'')]}}{4\pi r(z'')}\oint dc\, K_z(c) e^{jk(\rho/r)[x'(c)\cos\varphi + y'(c)\sin\varphi]}. \tag{12}$$

We consider the higher modes to be in deep cutoff, so that $kx'(c), ky'(c) \ll 1$, hence

$$A_z \approx \mu_0 e^{-jkz} \int_{z_1-z}^{z_2-z} dz'' \frac{e^{-jk[z''+r(z'')]}}{4\pi r(z'')} \oint dc\, K_z(c) \left\{1 + jk(\rho/r)[x'(c)\cos\varphi + y'(c)\sin\varphi]\right\}. \tag{13}$$

Separating the contour integral $\oint dc = \oint dc_1 + \oint dc_2$, where $c_{1,2}$ are the contours of the "upper" and "lower" conductors respectively, and using

$$\oint dc_1 K_z(c_1) = -\oint dc_1 K_z(c_2) = I_0 \tag{14}$$

so that the integral on each surface current distribution results in the total current, which is equal but with opposite signs on the conductors. We may define the 2D vector $\boldsymbol{\rho}(c) \equiv (x'(c), y'(c))$, from which one defines the vector distance between the center of the surface current distributions

$$\mathbf{d} \equiv \left[\oint dc_1 K_z(c_1)\boldsymbol{\rho}(c_1) + \oint dc_1 K_z(c_2)\boldsymbol{\rho}(c_2)\right] / I_0, \tag{15}$$

so that Eq. (13) may be written as

$$A_z = \mu_0 e^{-jkz} I_0 jk[d_x \cos\varphi + d_y \sin\varphi] \int_{z_1-z}^{z_2-z} dz'' \frac{e^{-jk[z''+r(z'')]}}{4\pi r(z'')} \frac{\rho}{r(z'')}, \tag{16}$$

where d_x and the d_y are the x and y components of the vector $\mathbf{d}$. This represents a 2D dipole approximation of the TL, so that it can be treated as a twin lead, as shown in Figure 2, and without loss of generality, one redefines the x axis to be aligned with $\mathbf{d}$, so that $d_x = d$ and $d_y = 0$, obtaining

$$A_z = \mu_0 e^{-jkz} I_0 jkd\cos\varphi \int_{z_1-z}^{z_2-z} dz'' \frac{e^{-jk[z''+r(z'')]}}{4\pi r} \frac{\rho}{r(z'')}, \tag{17}$$

which is equivalent of having a current confined on conductor 1 (at $x = d/2$)

$$I_1 = I_0 e^{-jkz}, \tag{18}$$

and a current confined on conductor 2 (at $x = -d/2$),

$$I_2 = -I_0 e^{-jkz} \tag{19}$$

representing a twin lead, where the requirement of ρ to be much bigger than the transverse dimensions, results in $\rho \gg d$.

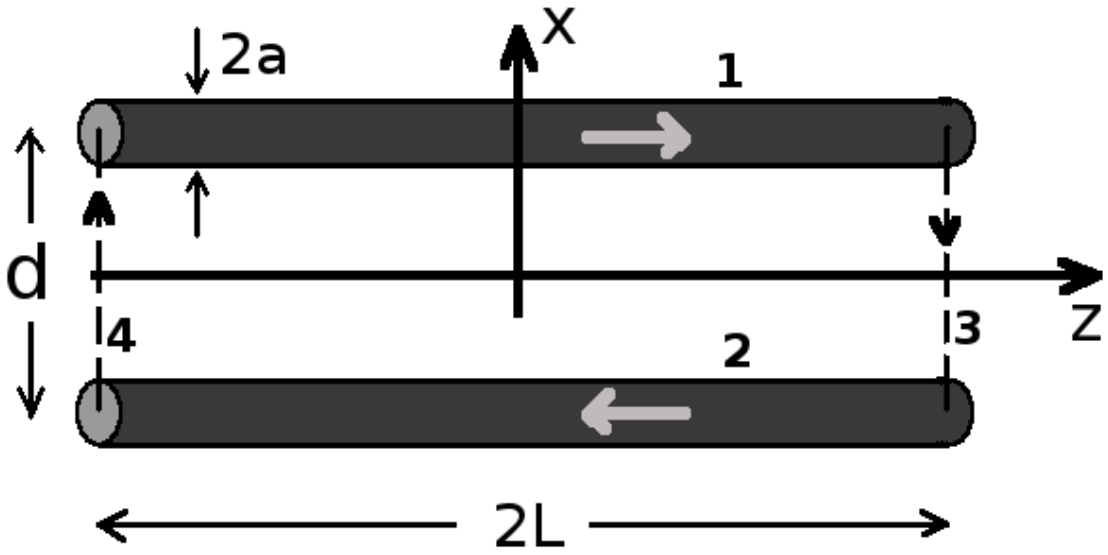

FIG. 2: The transmission line is modeled as a twin lead in free space, with distance d between the conductors. The currents in the transmission line flow in the z direction at $x = \pm d/2$ and they are defined as contributions 1 and 2 respectively to the magnetic vector potential A_z. The termination currents (source or load) flow in the x direction and are defined as contributions 3 and 4 to the magnetic vector potential A_x. The arrows on conductors 1,2,3 and 4 show the conventional directions of those currents. The radius of the wires is a, but it is relevant only for the characteristic impedance and not for the radiation. The length of the transmission line is $2L$ (but we also consider infinite or semi-infinite lines).

We are interested in radiation, so we require the observer to be many wavelengths far from the TL: $k\rho \gg 1$. Using this requirement, Eq. (17) may be further simplified to

$$A_z = -\frac{\mu_0 I_0 e^{-jkz} d\cos\varphi}{4\pi}\frac{\partial}{\partial\rho}\int_{z_1-z}^{z_2-z} dz'' \frac{e^{-jk[z''+r(z'')]}}{r(z'')}. \tag{20}$$

The dz'' integral results in the exponential integral function Ei as follows

$$A_z = -\frac{\mu_0 I_0 e^{-jkz} d\cos\varphi}{4\pi}\frac{\partial}{\partial\rho}\,\mathrm{Ei}\left(-jk\left[z'' + \sqrt{(z'')^2+\rho^2}\right]\right)\Bigg|_{z_1-z}^{z_2-z}, \tag{21}$$

where the Ei function satisfies $d\,\mathrm{Ei}(s)/ds = e^s/s$.

This twin lead model is used for all the cases we analyze: infinite TL, semi infinite TL and finite TL, as follows. The twin lead geometry also allows us to use simple models for the termination currents in the x direction, defining the x component of the magnetic vector potential.

IV. INFINITE TL ANALYSIS

In this section we consider an infinite twin lead TL, carrying a forward moving wave, so that we do not need to consider the termination currents, and we may use the result (21) with $z_1 = -\infty$ and $z_2 = \infty$. Replacing $z_1 - z = -L$ and $z_2 - z = L$, considering $L \to \infty$ we obtain

$$A_z = -\frac{\mu_0 I_0 e^{-jkz} d\cos\varphi}{4\pi}\frac{\partial}{\partial\rho}\left\{\mathrm{Ei}\left(-jk\left[L+\sqrt{L^2+\rho^2}\right]\right) - \mathrm{Ei}\left(-jk\left[-L+\sqrt{L^2+\rho^2}\right]\right)\right\}, \tag{22}$$

so that the integral itself does not converge, but we only need its derivative with respect to ρ. For $L \gg \rho$ the result is

$$A_z = -\frac{\mu_0 I_0 e^{-jkz} d\cos\varphi}{4\pi}\frac{\partial}{\partial\rho}\left\{\mathrm{Ei}(-jk2L) - \mathrm{Ei}\left(-jk\frac{\rho^2}{2L}\right)\right\}, \tag{23}$$

so that the constant $\mathrm{Ei}(-jk2L)$ does not contribute and in the limit $L \to \infty$ we obtain

$$A_z = \frac{\mu_0 I_0}{4\pi} d\cos\varphi \frac{2e^{-jkz}}{\rho} \tag{24}$$

from which

$$\mathbf{H} = \frac{1}{\mu_0}\boldsymbol{\nabla}\times\mathbf{A} = \frac{e^{-jkz}}{2\pi}\frac{I_0 d}{\rho^2}[-\widehat{\boldsymbol{\rho}}\sin\varphi + \widehat{\boldsymbol{\varphi}}\cos\varphi] \tag{25}$$

and

$$\mathbf{E} = \frac{1}{j\omega\epsilon_0}\boldsymbol{\nabla}\times\mathbf{H} = \eta_0\frac{e^{-jkz}}{2\pi}\frac{I_0 d}{\rho^2}[\widehat{\boldsymbol{\rho}}\cos\varphi + \widehat{\boldsymbol{\varphi}}\sin\varphi], \tag{26}$$

so that the Poynting vector is

$$\mathbf{S} = \mathbf{E}\times\mathbf{H}^* = \eta_0\frac{1}{4\pi^2}\frac{|I_0|^2 d^2}{\rho^4}\widehat{\mathbf{z}} \tag{27}$$

Clearly, an infinite line (even having the geometry of an open structure), never radiates in the usual sense, i.e. as an escaping power. Calculating here the "radiated" power just results in the power carried by the TL (this is true if the space around the TL is completely free of any objects that come in contact with the fields of the TL).

Therefore, any radiation from a TL must emerge from a termination, as we shall see in the next section in which we analyze a semi-infinite TL.

V. SEMI-INFINITE TL ANALYSIS

In this section we consider a semi-infinite twin lead TL, carrying a forward moving wave. Here we shall need also the contribution of the end current (conductor 3 in Figure 2), because

ignoring it violates the current continuity principle. But we first calculate the contribution of conductors 1 and 2 and hence we call it $A_{z\,1,2}$. The termination point is at $z=0$, so that we may use the result (21) with $z_1=-\infty$ and $z_2=0$. Replacing $z_1-z=-L$ and $z_2-z=-z$, considering $L\to\infty$ we obtain so the magnetic potential vector in the z direction

$$A_{z\,1,2}=-\frac{\mu_0 I_0 e^{-jkz}d\cos\varphi}{4\pi}\frac{\partial}{\partial\rho}\left\{\mathrm{Ei}\left(-jk\left[-z+\sqrt{z^2+\rho^2}\right]\right)-\mathrm{Ei}\left(-jk\left[-L+\sqrt{L^2+\rho^2}\right]\right)\right\}, \tag{28}$$

which for $L\gg\rho$ is rewritten as

$$A_{z\,1,2}=\frac{\mu_0 I_0 e^{-jkz}d\cos\varphi}{4\pi}\frac{\partial}{\partial\rho}\left\{\mathrm{Ei}\left(-jk\frac{\rho^2}{2L}\right)-\mathrm{Ei}\left(-jk\left[-z+\sqrt{z^2+\rho^2}\right]\right)\right\}, \tag{29}$$

which results in

$$A_{z\,1,2}=\frac{\mu_0 I_0}{4\pi}d\cos\varphi\left[\frac{2e^{-jkz}}{\rho}-\frac{\rho}{r-z}\frac{e^{jkr}}{r}\right]\equiv A_{z\,1,2\,\mathrm{plane}}+A_{z\,1,2\,\mathrm{spherical}}, \tag{30}$$

where $r=\sqrt{\rho^2+z^2}$ is the radial coordinate in spherical coordinates. The left expression describes the plane wave we received for the infinite line too, and the right expression describes a spherical wave emerging from the end of the transmission line at the coordinates origin.

At $z>0$, the plane wave and its singularity at $\rho=0$ has to disappear, and one can easily check that the spherical wave cancels it. For $\rho\ll z$, approximating the spherical wave to first order, we have $r\approx z+\frac{\rho^2}{2z}$, so that $r-z\approx\frac{\rho^2}{2z}$ and the spherical wave reduces to $-\frac{2e^{-jkz}}{\rho}$.

The radiated power may be calculated from the spherical wave, which is rewritten in spherical coordinates as

$$A_{z\,1,2\,\mathrm{spherical}}=\mu_0 F_{1,2}(\theta,\varphi)G(r), \tag{31}$$

We reintroduced here the definition of the Green's function from Eq. (5), and the directivity function $F_{1,2}$ is

$$F_{1,2}(\theta,\varphi)=-I_0 d\cos\varphi\frac{\sin\theta}{1-\cos\theta}, \tag{32}$$

We may calculate $\mathbf{H}=\frac{1}{\mu_0}\boldsymbol{\nabla}\times\mathbf{A}_{1,2\,\mathrm{spherical}}$ by approximating $\boldsymbol{\nabla}\simeq-jk\hat{\mathbf{r}}$, obtaining

$$\mathbf{H}_{1,2}=jkF_{1,2}(\theta,\varphi)\sin\theta G(r)\widehat{\boldsymbol{\varphi}}, \tag{33}$$

and the electric field comes out

$$\mathbf{E}_{1,2}=\eta_0 jkF_{1,2}(\theta,\varphi)\sin\theta G(r)\widehat{\boldsymbol{\theta}}, \tag{34}$$

Now we calculate the contribution of the end current (contribution 3 in Figure 2), which flows at $z = 0$ in the $-\widehat{x}$ direction, and is of magnitude I_0, giving rise to

$$A_{x\,3} = -\mu_0 I_0 \int_{-d/2}^{d/2} dx' G(R_3) \tag{35}$$

where

$$R_3 \simeq r - x' \sin\theta \cos\varphi \tag{36}$$

is the distance of the far observer from the end current at $z = 0$ and $-d/2 \leq x \leq d/2$. This results in

$$A_{x\,3} = \mu_0 F_3(\theta, \varphi) G(r), \tag{37}$$

where the directivity function F_3 is

$$F_3(\theta, \varphi) = -I_0 d\,\mathrm{sinc}\left(\frac{kd}{2}\sin\theta\cos\varphi\right) \simeq -I_0 d, \tag{38}$$

so that for $kd \ll 1$, the argument of the sinc function is very close to 0 for any angles θ and φ, so we approximate it by 1. Next we obtain

$$\mathbf{H}_3 = \frac{1}{\mu_0}\boldsymbol{\nabla} \times \mathbf{A}_3 \simeq \frac{1}{\mu_0}(-jk\widehat{\mathbf{r}}) \times (A_{x\,3}\widehat{\mathbf{x}}) \tag{39}$$

which comes out

$$\mathbf{H}_3 = -jk(\cos\theta\cos\varphi\widehat{\boldsymbol{\varphi}} + \sin\varphi\widehat{\boldsymbol{\theta}})G(r)F_3, \tag{40}$$

from which we calculate

$$\mathbf{E}_3 = \frac{1}{j\omega\epsilon_0}(-jk\widehat{\mathbf{r}}) \times \mathbf{H}_3 = \eta_0 jk(-\cos\theta\cos\varphi\widehat{\boldsymbol{\theta}} + \sin\varphi\widehat{\boldsymbol{\varphi}})G(r)F_3. \tag{41}$$

Adding up the fields we obtain

$$\mathbf{H} = \mathbf{H}_{1,2} + \mathbf{H}_3 = jkG(r)[\widehat{\boldsymbol{\varphi}}(F_{1,2}\sin\theta - F_3\cos\theta\cos\varphi) - \widehat{\boldsymbol{\theta}}F_3\sin\varphi] \tag{42}$$

and

$$\mathbf{E} = \mathbf{E}_{1,2} + \mathbf{E}_3 = \eta_0 jkG(r)[\widehat{\boldsymbol{\theta}}(F_{1,2}\sin\theta - F_3\cos\theta\cos\varphi) + \widehat{\boldsymbol{\varphi}}F_3\sin\varphi], \tag{43}$$

resulting in Poynting vector $\mathbf{E} \times \mathbf{H}^*$:

$$\mathbf{S} = \eta_0 \frac{k^2\widehat{\mathbf{r}}}{16\pi^2 r^2}(|F_{1,2}\sin\theta - F_3\cos\theta\cos\varphi|^2 + |F_3\sin\varphi|^2), \tag{44}$$

which results in

$$\mathbf{S} = \eta_0 \frac{(kd)^2\widehat{\mathbf{r}}}{16\pi^2 r^2}|I_0|^2, \tag{45}$$

So that the total radiated power is

$$P_{rad} = \int_0^{2\pi} \int_0^{\pi} \sin\theta d\theta d\varphi r^2 \widehat{\mathbf{r}} \cdot \mathbf{S} = \eta_0 \frac{(kd)^2}{4\pi} |I_0|^2 \tag{46}$$

Clearly, this result shows that any TL radiates only from its terminations, specifically the semi-infinite line radiates from its end. It therefore looks like the radiation process forms in a region near the termination in analogy with Optical Transition Radiation (OTR) as a *formation length* [6, 7].

A. Non matched line

In case the TL is not matched we have to deal with a forward an backward wave. The backward wave is defined as in Eqs. (18) and (19), only e^{-jkz} is replaced by e^{jkz}. Defining the complex amplitude of the backward wave I_b, after some algebra, we find that a backward wave results in the z directed magnetic potential vector

$$A_{z\,1,2\,b} = \frac{\mu_0 I_b}{4\pi} d \cos\varphi \frac{\rho}{r+z} \frac{e^{jkr}}{r} \tag{47}$$

where the subscript "b" means backward. The plane wave can be recovered from (47) for negative z which satisfies $|z| \gg \rho$ by approximating the spherical wave to first order, so that $r \approx |z| + \frac{\rho^2}{2|z|}$. The spherical wave reduces in this conditions to $\frac{2e^{jkz}}{\rho}$, recovering the plane wave in Eq. (30), only traveling to the left.

Therefore for a backward wave $F_{1,2}$ in Eq. (32) has an opposite sign with $cos\theta$ replaced by $-cos\theta$, so that

$$F_{1,2\,b}(\theta, \varphi) = I_b d \cos\varphi \frac{\sin\theta}{1+\cos\theta}, \tag{48}$$

The end current is the same as for the forward wave, only replace I_0 by I_b, hence F_3 is similar to (38):

$$F_{3\,b}(\theta, \varphi) = -I_b d, \tag{49}$$

To calculate the power radiated by both waves, we have to replace $F_{1,2} \to F_{1,2} + F_{1,2\,b}$ and $F_3 \to F_3 + F_{3\,b}$ in Eq. (44), and the result is

$$\mathbf{S} = \eta_0 \frac{(kd)^2 \widehat{\mathbf{r}}}{16\pi^2 r^2} \left(|I_0|^2 + |I_b|^2 \right). \tag{50}$$

This means that separate forward or backward waves have the same radiation, or in other words a wave traveling into the termination or out of it radiates the same. We also see that

the interference between the waves does not contribute to the radiation, so that the powers radiated by the separate waves is added up.

To examine how the radiation forms as function of the distance from the termination we analyze in the next section a finite twin lead transmission line.

VI. FINITE TL ANALYSIS

We consider in this section a finite twin lead transmission line, of length $2L$, from $z=-L$ to $z=L$, carrying a forward moving wave. Before calculating, we understand from the conclusions of the previous section that for a long enough TL, we can look at it as one termination (the source) sending out a wave which is received by the other termination (the load). A wave exiting from a termination or entering into a termination radiates according to Eq. (46) and in this case both waves have the same amplitude I_0, so one forward wave has to result in twice the result of Eq. (46)

$$P_{rad\ \text{(long finite TL)}} = 2\times\eta_0\frac{(kd)^2}{4\pi}|I_0|^2 = \eta_0\frac{(kd)^2}{2\pi}|I_0|^2, \tag{51}$$

and we shall confirm this result for big L.

To calculate the magnetic vector potential for the finite TL we may use the result (21), but it will be quicker for to do the calculations from scratch.

There are four currents contributing to the radiation: currents 1 and 2 contribute to the z component of the magnetic potential vector and currents 3 and 4 contribute to the x component of the magnetic potential vector, see Figure 2 (contribution 3 and 4 have been neglected in [1], therefore the result obtained there was not accurate).

We start with currents 1 and 2, defined in Eqs. (18) and (19). The distances of a far observer from the conductors carrying those currents are

$$R_{1,2}\simeq r - z'\cos\theta \mp (d/2)\sin\theta\cos\varphi, \tag{52}$$

and they contribute to the z directed vector potential

$$A_{z\,1,2} = \mu_0 I_0\int_{-L}^{L} dz' e^{-jkz'}(G(R_1)-G(R_2)) \tag{53}$$

where $G(s)$ is defined in Eq. (5) is the 3D Green's function. The result of integral (53) in the far field is

$$A_{z\,1,2} = \mu_0 G(r)F_{1,2}(\theta,\varphi) \tag{54}$$

where

$$F_{1,2}(\theta,\varphi) = jI_0 2Lkd\sin\theta\cos\varphi\,\mathrm{sinc}\left(\frac{kd}{2}\sin\theta\cos\varphi\right)\mathrm{sinc}\left[kL(1-\cos\theta)\right] \tag{55}$$

is the radiation function from contributions 1 and 2, and the "sinc" function is defined in Eq. (3). In the far field, the $\boldsymbol{\nabla}$ operator is approximated by $-jk\widehat{\mathbf{r}}$ and one obtains the far $\mathbf{H}$ field

$$\mathbf{H}_{1,2} = \frac{1}{\mu_0}\boldsymbol{\nabla}\times\mathbf{A}_{1,2} = jkG(r)F_{1,2}(\theta,\varphi)\sin\theta\widehat{\boldsymbol{\varphi}} \tag{56}$$

and the far $\mathbf{E}$ field is obtained by

$$\mathbf{E}_{1,2} = \frac{1}{j\omega\epsilon_0}\boldsymbol{\nabla}\times\mathbf{H}_{1,2} = \eta_0 jkG(r)F_{1,2}(\theta,\varphi)\sin\theta\widehat{\boldsymbol{\theta}}, \tag{57}$$

where $\eta_0 = \sqrt{\mu_0/\epsilon_0}$ is the free space impedance.

Next we consider the contributions 3 and 4

$$I_3(x) = -I_0 e^{-jkL} \tag{58}$$

flowing at $(z = L, y = 0)$ in the $-x$ direction, and

$$I_4(x) = I_0 e^{jkL} \tag{59}$$

flowing at $(z = -L, y = 0)$ in the x direction. Both I_3 and I_4 are fixed and don't depend on x. The distances of a far observer from those currents is

$$R_{3,4} \simeq r \mp L\cos\theta - x'\sin\theta\cos\varphi. \tag{60}$$

Those currents contribute to a x directed vector potential

$$A_{x\,3,4} = \mu_0 I_0 \int_{-d/2}^{d/2} dx'(e^{jkL}G(R_4) - e^{-jkL}G(R_3)) \tag{61}$$

The result of integral (61) in the far field is

$$A_{x\,3,4} = \mu_0 G(r)F_{3,4}(\theta,\varphi) \tag{62}$$

where

$$F_{3,4}(\theta,\varphi) = jI_0 dk2L(1-\cos\theta)\,\mathrm{sinc}\left[kL(1-\cos\theta)\right]\mathrm{sinc}\left(\frac{kd}{2}\sin\theta\cos\varphi\right) \tag{63}$$

is the radiation function from contributions 3 and 4. One obtains the far $\mathbf{H}$ field

$$\mathbf{H}_{3,4} = \frac{1}{\mu_0}\boldsymbol{\nabla} \times \mathbf{A}_{3,4} = -jkG(r)F_{3,4}(\cos\theta\cos\varphi\widehat{\boldsymbol{\varphi}} + \sin\varphi\widehat{\boldsymbol{\theta}}) \tag{64}$$

and the far $\mathbf{E}$ field is obtained by

$$\mathbf{E}_{3,4} = \frac{1}{j\omega\epsilon_0}\boldsymbol{\nabla} \times \mathbf{H}_{3,4} = \eta_0 jkG(r)F_{3,4}(\sin\varphi\widehat{\boldsymbol{\varphi}} - \cos\theta\cos\varphi\widehat{\boldsymbol{\theta}}). \tag{65}$$

The total $\mathbf{H} = \mathbf{H}_{1,2} + \mathbf{H}_{3,4}$ comes out

$$\mathbf{H} = jkG(r)[\widehat{\boldsymbol{\varphi}}(F_{1,2}\sin\theta - F_{3,4}\cos\theta\cos\varphi) - \widehat{\boldsymbol{\theta}}F_{3,4}\sin\varphi] \tag{66}$$

and the total $\mathbf{E} = \mathbf{E}_{1,2} + \mathbf{E}_{3,4}$ comes out

$$\mathbf{E} = \eta_0 jkG(r)[\widehat{\boldsymbol{\theta}}(F_{1,2}\sin\theta - F_{3,4}\cos\theta\cos\varphi) + \widehat{\boldsymbol{\varphi}}F_{3,4}\sin\varphi] \tag{67}$$

The far Poynting vector is

$$\mathbf{S} = \mathbf{E} \times \mathbf{H}^* = \eta_0\frac{k^2\widehat{\mathbf{r}}}{16\pi^2 r^2}(|F_{1,2}\sin\theta - F_{3,4}\cos\theta\cos\varphi|^2 + |F_{3,4}\cos\theta\cos\varphi|^2), \tag{68}$$

which comes out

$$\mathbf{S} = \widehat{\mathbf{r}}\eta_0\frac{k^4(2L)^2d^2|I_0|^2}{16\pi^2 r^2}(1-\cos\theta)^2\,\mathrm{sinc}^2\left(\frac{kd}{2}\sin\theta\cos\varphi\right)\mathrm{sinc}^2\left[kL(1-\cos\theta)\right] \tag{69}$$

so that the total radiated power is

$$P_{rad} = \int_0^{2\pi}\int_0^{\pi}\sin\theta d\theta d\varphi r^2\widehat{\mathbf{r}}\cdot\mathbf{S} \tag{70}$$

As mentioned before, we consider frequencies for which TE/TM modes are in deep cutoff, so that $kd \ll 1$. We therefore approximate $\mathrm{sinc}^2\left(\frac{kd}{2}\sin\theta\cos\varphi\right) \simeq 1$, so that the integrand in (70) is not a function of φ, obtaining

$$P_{rad} = \frac{\eta_0(kd)^2|I_0|^2}{2\pi}\left[1 - \mathrm{sinc}(4kL)\right], \tag{71}$$

which for $2L$ bigger than a few wavelengths confirms the expected result in Eq. (51), so that for a fixed frequency, the radiated power goes to a constant when increasing the TL length $2L$:

$$\lim_{L\to\infty} P_{rad} = \frac{\eta_0(kd)^2|I_0|^2}{2\pi}. \tag{72}$$

This constant is exactly twice the power radiated from the semi-infinite TL, and in practice this limit is reached at around few wavelengths. This means that for a longer line, only the last wavelengths at the end of the TL radiate, and this last wavelengths can be understood in analogy with Optical Transition Radiation (OTR) as a *formation length* [6, 7].

A. Non matched line

The results of non matched line analysis we did for the semi-infinite TL, apply also to the finite TL, so that calling again the amplitudes of the forward and backward waves I_0 and I_b, the result (71) becomes

$$P_{rad} = \frac{\eta_0 (kd)^2}{2\pi} \left(|I_0|^2 + |I_b|^2 \right) \left[1 - \mathrm{sinc}(4kL) \right], \tag{73}$$

showing again that the interference between the waves does not contribute to the radiation, so that the powers radiated by the forward or backward waves add up.

VII. COMPARISON WITH SIMULATIONS

We shall compare with simulation the ratio between the radiated power and the power to the load:

$$\frac{P_{rad}}{P^+} = \frac{\eta_0}{Z_0} \frac{(kd)^2}{2\pi} \left[1 - \mathrm{sinc}(4kL) \right]. \tag{74}$$

where $Z_0 = \frac{\eta_0}{\pi} \ln(d/a)$ is the characteristic impedance of this twin lead TL.

We simulated the configuration in Figure 2 using ANSYS-HFSS commercial software, in the frequency domain, FEM technique. We ran the simulation at a fixed frequency of 240 MHz, using $d = 2.54$ cm, $d/a = 7.91$ and obtained S matrices defined for a characteristic impedance of $R = 257.4\Omega$ at both ports, for different lengths of the transmission line. By symmetry, the S matrix has the form

$$S = \begin{pmatrix} \Gamma & \tau \\ \tau & \Gamma \end{pmatrix}, \tag{75}$$

from which one may calculate the ABCD matrix of the TL [2, 12, 13], using

$$A = D = \frac{1}{2} \left[\tau + (1 - \Gamma^2)/\tau \right] \tag{76}$$

$$B = \frac{R}{2} \left[-\tau + (1 + \Gamma)^2/\tau \right] \tag{77}$$

$$C = \frac{1}{2R} \left[-\tau + (1 - \Gamma)^2/\tau \right] \tag{78}$$

from which we compute the delay angle of the TL

$$\Theta = \arccos(A) \tag{79}$$

and the characteristic impedance

$$Z_0 = \sqrt{B/C} \tag{80}$$

The radiated power, relative to the load power is obtained by

$$\frac{P_{rad}}{P^+} = -2Im\{\Theta\}, \tag{81}$$

and $Im\{\Theta\} < 0$ always. In Figure 3 we compare the analytic result in Eq. (74) with the result obtained from simulation Eq. (81). We see that the simulation overestimates the

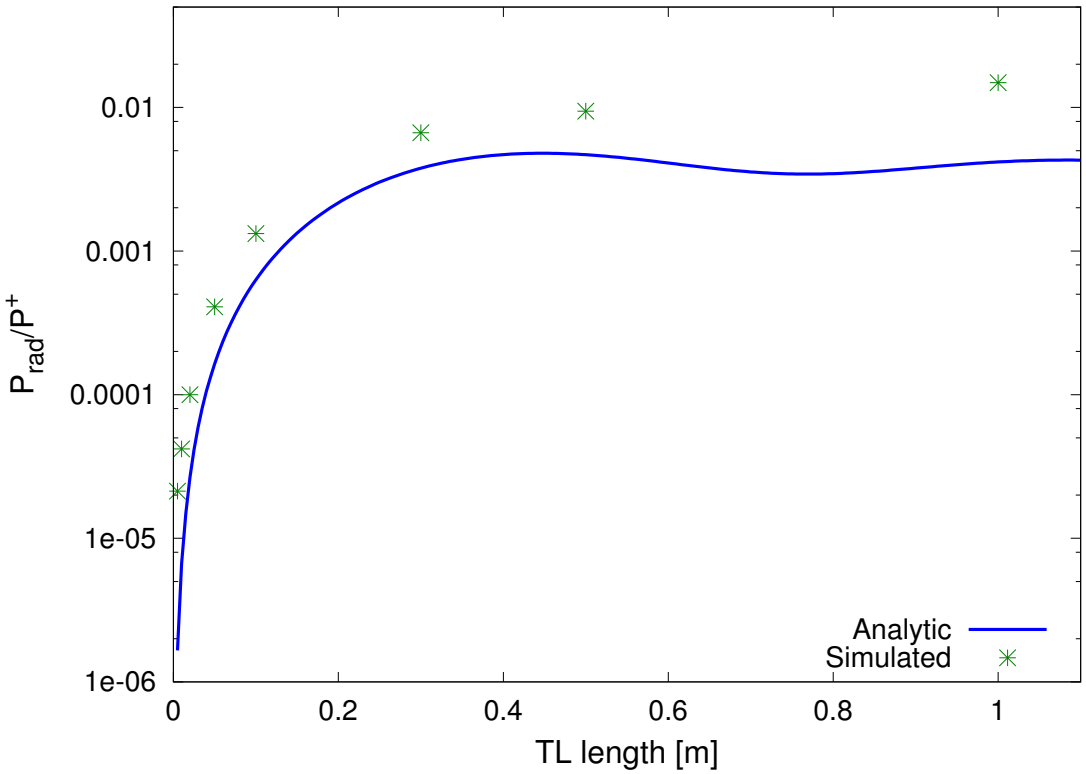

FIG. 3: Relative radiation losses P_{rad}/P^+: comparison between the analytic result in Eq. (74) and the simulation result in Eq. (81).

radiation losses, but shows the general tendency of the radiation losses as function of the TL length, proving that this theory is reliable. We still have to improve the simulation accuracy to handle smaller radiation losses, however the good comparison between the finite and semi-infinite TL increases our confidence that the theoretical result is correct.

VIII. RADIATION MODEL FOR TL

The radiation process can be incorporated in the RLCG model, either by a series resistance per length unit R or by a parallel conductance per length unit G. This radiation element in the model represents the power loss per TL length unit due to radiation. For a wave moving forward in the z direction, the power carried by the wave should decrease with z, so that $-dP/dz = |I_0|^2 R$ in case of the serial representation or $-dP/dz = |V_0|^2 G$ in case of the parallel representation.

Both representations are possible, and the question is which one is the more adequate. Using the Lorenz gauge in the frequency domain we have

$$\boldsymbol{\nabla} \cdot \mathbf{A} + \frac{j\omega}{c^2} V = 0. \tag{82}$$

Under the Lorenz gauge, the magnetic vector potential $\mathbf{A}$ and the electric scalar potential V satisfy wave equations with separate excitations $\mathbf{J}$ and ρ, respectively:

$$\left(\nabla^2 + k^2\right) \mathbf{A} = -\mu_0 \mathbf{J} \tag{83}$$

and

$$\left(\nabla^2 + k^2\right) V = -\rho/\epsilon_0. \tag{84}$$

The solution of Eq. (83) is the convolution integral with the Green's function, like the integral in Eq. (53) for example. The solution of Eq. (84) is similar, only use the charge density per length unit (λ) on the TL instead of the current (I). Given the current continuity equation $\partial I/\partial z + j\omega\lambda = 0$, λ can be derived from I, and so the scalar potential V can be derived from the magnetic vector potential $\mathbf{A}$ via the Lorenz gauge (82), making Eq. (84) redundant. However, it is worthwhile to understand which part of the electric field, which can be expressed by

$$\mathbf{E} = -j\omega\mathbf{A} - \boldsymbol{\nabla} V \equiv \mathbf{E}_I + \mathbf{E}_\lambda \tag{85}$$

is due to the current and which part is due to the charges. The first part $\mathbf{E}_I = -j\omega\mathbf{A}$ is due to the current and the second part $\mathbf{E}_\lambda = -\boldsymbol{\nabla} V$ is due to the charges. For z directed currents, so that $\mathbf{A} = A_z \widehat{\mathbf{z}}$, we can work out this two parts, using for the far field $\boldsymbol{\nabla} \simeq -jk\widehat{\mathbf{r}}$ and using the Lorenz gauge, obtaining

$$\mathbf{E}_I = -j\omega A_z (\widehat{\mathbf{r}} \cos\theta - \widehat{\boldsymbol{\theta}} \sin\theta) \tag{86}$$

and

$$\mathbf{E}_\lambda = j\omega A_z \widehat{\mathbf{r}} \cos\theta, \tag{87}$$

so that their sum is in the $\widehat{\boldsymbol{\theta}}$ direction as it should. But we see that while $\mathbf{E}_I$ has a $\widehat{\boldsymbol{\theta}}$ component, $\mathbf{E}_\lambda$ is entirely directed toward $\widehat{\mathbf{r}}$, so that it does not contribute to the $\widehat{\mathbf{r}}$ directed Poynting vector.

The conclusion from this analysis is that the radiation is due to the current, so that the serial representation is the correct one. An additional argument in favor of this choice is the "self force" (or damping force) on radiating charges [8–11] which is co-linear with the charges acceleration so that it may be represented by a serial resistor.

Hence, we model the radiation by a serial resistance per length unit R in the RLCG model. The radiation being attributed to the terminations of the TL, the radiation model is symmetric around the middle of the line (at $z = 0$), we shall therefore examine how half of P_{rad} in Eq. (71) changes with half the TL length L.

The radiation resistance per length unit R, satisfies

$$\frac{d(P_{rad}/2)/dL}{P^+} = \frac{\eta_0}{Z_0}\frac{(kd)^2}{4\pi L}\left[\mathrm{sinc}(4kL) - \cos(4kL)\right] = \frac{R(L)}{Z_0}. \tag{88}$$

For the model to be applicable to a semi-infinite TL, it has to start at the termination point. We define s the distance from the termination of the TL (for example if we deal with a semi-infinite TL which terminates at $z = 0$, we have $s = -z$, for $0 \le s < \infty$). The value of $R(L)$ in Eq. (88) is expressed as function of s as follows

$$R(s) = \frac{\eta_0 (kd)^2}{4\pi s}\left[\mathrm{sinc}(4ks) - \cos(4ks)\right] \tag{89}$$

The behavior of the normalized $R(s)$ for a semi-infinite TL is shown in Figure 4. This model reproduces the correct radiation power, since

$$|I_0|^2 \int_0^\infty R(s)ds = \eta_0 \frac{(kd)^2}{4\pi}|I_0|^2 \tag{90}$$

Clearly, to describe the correct radiation losses, $R(s)$ must also have negative values, due to the oscillatory behavior of the radiated power as function of the TL length. But this does not represent any problem, because the overall losses come out always positive.

For a finite TL, we set $R(s)$ in Eq. (89) from each side up to the middle of the TL. Hence if the TL length is $2L$, $0 \le s \le L$ from each side, as shown in Figure 5 and the model

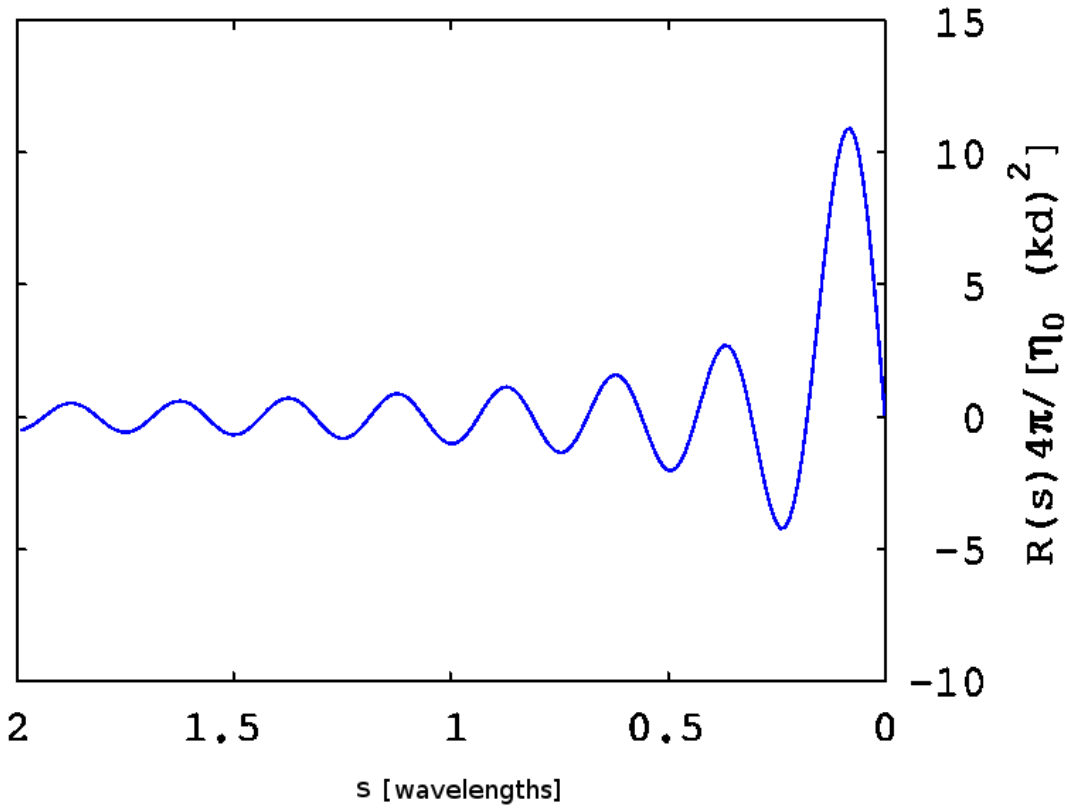

FIG. 4: Normalized value of the radiation resistance per length unit $R(s)$ for a semi-infinite transmission line ending at $z = 0$. The parameter s is the distance from the TL termination point, and $R(s)$ is linear with s for small s. For big s it oscillates around 0 till it practically becomes 0 far from the termination of the TL.

describes correctly the radiation power since

$$|I_0|^2 \int_{-L}^{L} R(s)ds = 2|I_0|^2 \int_0^L R(s)ds = \frac{\eta_0 (kd)^2 |I_0|^2}{2\pi} [1 - \mathrm{sinc}(4kL)] \tag{91}$$

Unlike in the case of ohmic or dielectric losses, for which the RLCG losses model is accurate only for a separate forward or backward wave, the radiation model is accurate for any combination of waves, because as we saw in the previous sections, the interference between the waves does not contribute to the radiation.

IX. CONCLUSIONS

We showed in this work that radiation losses in TL originate from the current in the region of several wavelengths near the termination(s) of the TL (in analogy with OTR [6, 7]), so

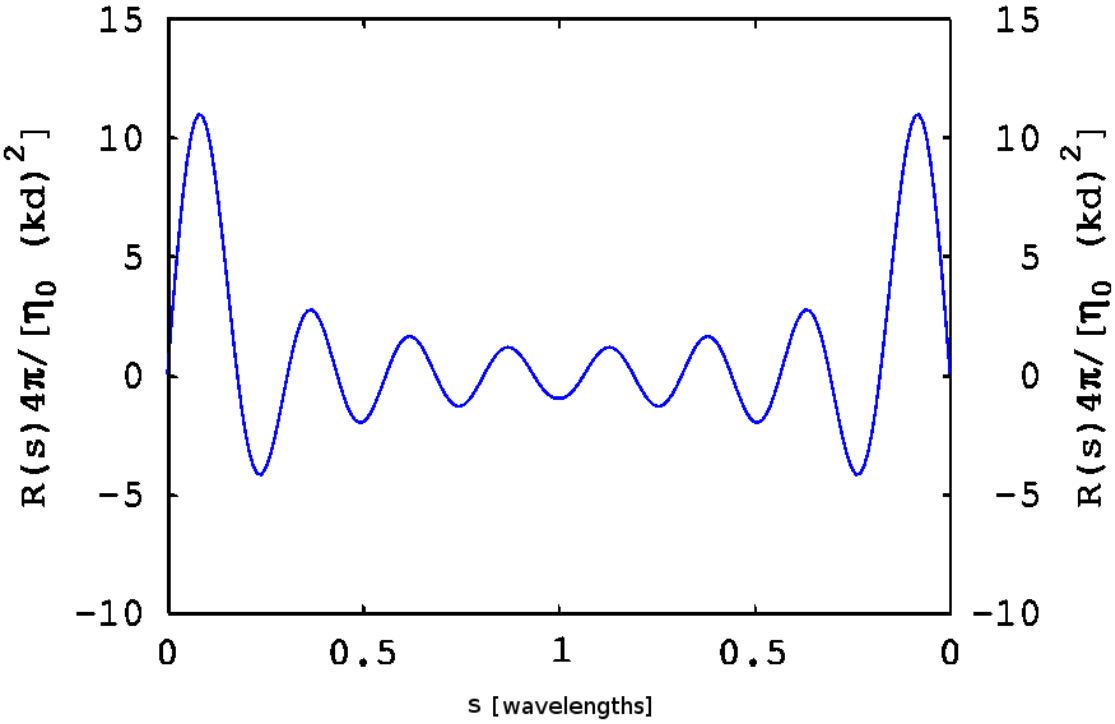

FIG. 5: Same as in Figure 4, only that for a finite TL of length $2L$, s measures the distance from each termination, up to the middle of the line, so that $0 \leq s \leq L$. In this example, L is one wavelength.

that one cannot properly define a "per length radiated power".

However, we where able to conceive a radiation model based on a variable radiation resistance per length unit $R(s)$, where s measures the distance from each termination up to the middle of the TL (or from the termination to infinity for a semi-infinite TL).

Unlike in the case of ohmic or dielectric losses, for which the R or G models respectively are accurate only for a separate forward or backward wave, the radiation model is accurate for any combination of current waves, because the interference between the waves does not contribute to the radiation.

Further work to be done: generalize the radiation model for TL inside a dielectric insu-

lator, and generalize the radiation model for multiconductor transmission lines (MTL).

---

[1] R. Ianconescu and V. Vulfin, *TEM Transmission line radiation losses analysis*, EUMW 2016, London, October 3-7 (2016)

[2] D. M. Pozar, *Microwave Engineering*, Wiley India Pvt., 2009

[3] Orfanidis S.J., *Electromagnetic Waves and Antennas*, ISBN: 0130938556, (Rutgers University, 2002)

[4] A. Gover, R. Ianconescu, C. Emma, P. Musumeci and A. Friedman, *Conceptual Theory of Spontaneous and Taper-Enhanced Superradiance and Stimulated Superradiance*, FEL 2015 Conference, August 23-28, Daejeon, Korea, 2015

[5] R. Ianconescu, E. Hemsing, A. Marinelli, A. Nause and A. Gover, *Sub-Radiance and Enhanced-Radiance of undulator radiation from a correlated electron beam*, FEL 2015 Conference, August 23-28, Daejeon, Korea, 2015

[6] A. Nause, E. Dyunin, R. Ianconescu and A. Gover, *Exact Theory of Optical Transition Radiation in the Far and Near Zones*, JOSA B, 31(10), pp. 2438-2445, (2014).

[7] V. L. Ginzburg, *Transition radiation and transition scattering*, Physica Scripta Volume T, 2:182, June 1982.

[8] R. Ianconescu, *Radiation from charges in the continuum limit* , AIP Advances, 3 (6), (2013)

[9] R. Ianconescu and L. P. Horwitz, *Energy mechanism of charges analyzed in real current environment*, Foundations of Physics Letters, Vol. 16, Number 3, pp. 225-244 (2003).

[10] R. Ianconescu and L. P. Horwitz, *Self-Force of a Charge in a Real Current*, Foundations of Physics Letters, Vol. 15, Number 6, pp. 551-559 (December 2002).

[11] R. Ianconescu and L.P. Horwitz, *Self-force of a classical charged particle*, Physical Review A, Vol. 45, Number 7, pp. 4346, (1992).

[12] V. Vulfin and R. Ianconescu, *Transmission of the maximum number of signals through a Multi-Conductor transmission line without crosstalk or return loss: theory and simulation*, IET MICROW ANTENNA P, 9(13), pp. 1444-1452 (2015)

[13] R. Ianconescu and V. Vulfin, *Simulation for a Crosstalk Avoiding Algorithm in Multi-Conductor Communication*, 2014 IEEE 28-th Convention of Electrical and Electronics Engineers in Israel, Eilat, December 3-5, (2014)